DEFENCE R&D DÉFENSE

Combining Head Models with Composite Models to Simulate Ballistic Impacts

J. van Hoof, M.J. Worswick
Department of Mechanical Engineering
University of Waterloo, Waterloo, Canada

Contract Serial Number:
W7701-8-1713/001/XSK

Submitted to

Dr. Kevin. Williams
DREV Canada

DISTRIBUTION STATEMENT A
Approved for Public Release
Distribution Unlimited

Defence R&D Canada

Defence Research Establishment Valcartier

Contract Report
DREV CR 2000-160
June 2001

National Defence Défense nationale

Canada

Combining Head Models with Composite Helmet Models to Simulate Ballistic Impacts

Final Report

DSS File Number XSK-8-00437 (305)

Contract Serial Number W7701-8-1713/001/XSK

November 30, 2000

DREV CR 2000-160

Submitted to

Dr. Kevin Williams

Defence Research Establishment Valcartier

Val-Belair, Quebec, Canada

By

J. van Hoof, M.J. Worswick

Department of Mechanical Engineering

University of Waterloo, Waterloo, Canada

PREFACE

This report is prepared in compliance with a Research Contract between the University of Waterloo and the Defence Research Establishment Valcartier (DREV). This document may contain proprietary information and shall not be disclosed, in whole or in part, to outside agencies or individuals without the written permission of the authors and DREV. The opinions expressed herein are those of the authors and do not necessarily represent those of the Defence Research Establishment Valcartier.

ABSTRACT

Numerical modelling of a helmeted head undergoing ballistic impact has been undertaken using a number of finite element codes and models. The composite helmet model developed at the University of Waterloo has been combined with a model of the human head, originally developed for automotive crash studies and extended to consider trauma due to ballistic impact by ESI and the Délégation Générale pour l'Armement (DGA). Conversion of the Waterloo helmet model from the VEC-DYNA format, in which it was originally developed, to the PAM-CRASH code format were unsuccessful because of incompatibilities between the Waterloo composite damage model's treatment of delamination damage and the PAM-CRASH contact surface implementation. With the DGA's permission, the DGA head model was successfully converted to the VEC-DYNA. Simulations were performed using the combined helmet and head model to obtain preliminary predictions of the behind armour blunt trauma resulting from projectile impacts on the helmet. The threat considered was a 1.1 g FSP impacting the front of the helmet at 586 m/s. Results from the simulations included contact forces and head accelerations resulting from the impact of the delaminated back plane of the composite helmet with the skull. Inadequate refinement of the existing head mesh in the vicinity of the impact sites was shown to limit the accurate prediction of the local contact conditions.

RÉSUMÉ

Des simulations numériques de la tête coiffée d'un casque composite sujet à des impacts balistiques ont été faites avec des codes et des modèles par éléments finis. Le modèle du casque composite développé par l'Université de Waterloo a été jumelé à un modèle de tête humaine, mis au point à l'origine par la société ESI et la Délégation Générale pour l'Armement (DGA) pour les besoins d'études de choc de l'industrie automobile et modifié pour inclure l'effet traumatique causé par l'impact de projectiles balistiques. Le transfert du modèle de casque de Waterloo, écrit à l'origine en format VEC-DYNA, au code PAM-CRASH de la société ESI n'a pas fonctionné en raison d'une incompatibilité entre le traitement de la délamination du modèle d'endommagement de composite de Waterloo et du modèle de contact de surface de PAM-CRASH. Avec l'autorisation de la DGA, le model de tête a donc été converti en VEC-DYNA avec succès. Des simulations ont donc été exécutées pour le modèle combiné tête/casque afin de d'obtenir des données préliminaires sur l'effet arrière résultant d'un projectile balistique qui frappe un casque. La menace étudiée consiste en un fragment simulé de 1,1 g qui frappe le devant d'un casque à une vitesse de 586 m/s. Les résultats de la simulation numérique nous donnent la force de contact et l'accélération de la tête causée par l'impact du plan intérieur du casque composite délaminé sur le crâne. Le maillage inadéquat du modèle de tête autour du point d'impact limite la précision des prévisions des conditions de contact local.

EXECUTIVE SUMMARY

Current testing standards for ballistic composite helmets focus on the prevention of projectile penetration, while the deformation of the laminate is generally ignored. However, the current consensus from research on the ballistic impact response of laminated helmets is that even in a non-perforating impact the helmet wearer can still suffer serious head injuries resulting from contact with the delaminated helmet interior. To support further optimisation of the ballistic performance of laminated helmets, an improved understanding of the nature of the delamination process of the helmet interior and its subsequent impact with the head of the helmet wearer is required.

The University of Waterloo composite damage model, designed to predict the penetration and delamination response of ballistically impacted laminated panels, has been successfully applied to predict the ballistic response of composite helmets using the VEC-DYNA finite element hydrocode. In order to investigate the behind armour blunt trauma associated with non-perforating impacts on the helmet, the numerical model of a PASGT helmet was combined with a head model provided by the French Délégation Générale pour l'armement (DGA). Since the DGA head model was formatted to run within the PAM-CRASH finite element code, the Waterloo composite damage model needed to be implemented within PAM-CRASH to enable collaborative exchange with the DGA. However, PAM-CRASH was found incapable of representing delaminations and modifications to remedy this problem have not been made available by ESI to date.

With the permission of the DGA, the University of Waterloo converted the head model to VEC-DYNA format as a work-around to the problems encountered in PAM-CRASH. Once the conversion was completed, it was possible to perform simulations of ballistic impacts on the combined helmet-head model and preliminary predictions of the contact forces resulting from the impact of the backplane with the skull have been obtained.

At present, the existing head model requires mesh refinement in the vicinity of the impact sites to accurately capture local contact conditions. There is also a need to migrate the Waterloo composite damage model from VEC-DYNA to the more advanced proprietary version of LS-DYNA. The skull re-meshing task is underway in follow-on work in an internally funded project at Waterloo while a joint project with UBC under DREV funding will address the delamination interface implementation in LS-DYNA.

SOMMAIRE

Les méthode de tests balistiques actuelles pour les casques en matériaux composites mettent l'accent sur la prévention de la pénétration des projectiles alors que la déformation et la délamination sont généralement peu étudiées. Cependant, il y a un consensus en recherche qui reconnaît qu'un impact balistique sur un casque laminé même non perforé, peut résulter en un contact à la tête causé par la délamination des couches intérieurs du casque qui peut provoquer un traumatisme sérieux. Afin d'optimiser les performances balistiques des casques en laminé du futur, une meilleure compréhension de la nature du processus de délamination des couches intérieures des casques et des impacts subséquents avec la tête est nécessaire.

Le modèle d'endommagement de composite de l'Université de Waterloo conçu pour prédire la réponse en pénétration et en délamination de structure laminée sollicitée par un impact en balistique, a été utilisé avec succès pour prédire la réponse balistique d'un casque en composite. Le modèle utilise la plate-forme d'éléments finis par hydrocode VEC-DYNA. Afin de pouvoir étudier le traumatisme causé par l'effet arrière d'une armure, en l'occurrence l'impact non perforant d'un casque composite, le modèle numérique du casque PASGT a été combiné au le modèle de tête mis au point par la Délégation Générale Française pour l'armement (DGA). Afin de bénéficier du modèle de tête mis au point pour fonctionner dans le code PAM-CRASH et de permettre une collaboration fructueuse avec la DGA, le modèle composite de l'Université de Waterloo devait être incorporé dans le code PAM-CRASH. Malheureusement, le code PAM-CRASH n'a pas permis la représentation adéquate du processus de délamination et les modifications requises pour corriger le problème n'ont pas été rendues disponibles à ce jour par la société ESI, propriétaire du code PAM-CRASH. Afin de contourner le problème lié au code PAM-CRASH et avec la permission de la DGA, l'Université de Waterloo a converti le modèle de tête pour le rendre opérationnel dans le code VEC-DYNA. Une fois ce travail effectué, il a été possible de faire les premières simulations d'impact balistique des modes combinés tête-casque et de faire des prédictions préliminaires sur les forces de contact résultant de l'impact de la déformation du plan arrière d'un casque avec le crâne.

Les travaux futurs nécessitent un raffinement du maillage autour du point d'impact pour obtenir précisément les conditions locales de contact. Il faut également faire le transfert du modèle d'endommagement des composites de Waterloo du code VEC-DYNA vers la version du code plus récente et plus performante, c.-à-d. LS-DYNA. Le remaillage du crâne est en cours à l'Université de Waterloo et un projet conjoint entre celle-ci et l'Université de Colombie-Britannique (UBC) est en cours pour faire l'interface du modèle de délamination de VEC-DYNA vers LS-DYNA.

TABLE OF CONTENTS

LIST OF TABLES

LIST OF FIGURES

1. INTRODUCTION

1.1 MOTIVATION

Helmets designed to protect the head under ballistic impact are commonly fabricated from laminated composites. Research into the ballistic impact response of laminated materials is still mainly empirical in nature. This empirical approach results in high costs involved in the design and testing of improved protection against more severe threats and in the application of new materials. Current testing standards for ballistic helmets focus on the prevention of projectile penetration, while the deformation of the laminate is generally ignored.

However, the current consensus from research on the ballistic impact response of laminated helmets is that the deformation of the composite is of vital importance. When helmets are impacted at velocities close to the ballistic limit, complete perforation might be prevented, but the projectile's kinetic energy can be sufficient to separate the inner, non-perforated laminate layers from the remainder of the helmet. This separation of the helmet interior is a delamination process and the delaminated layers are generally referred to as the backplane. Therefore, even though the helmet is not perforated, the helmet wearer can still suffer head injuries from the impact of the delaminated backplane with the head.

To support further optimisation of the ballistic performance of laminated helmets, an improved understanding of the nature of the backplane delamination process and the subsequent impact of the backplane with the head of the helmet wearer is required. The complex response of composite materials to ballistic impact, together with the high cost of instrumented ballistic impact tests would render a completely experimental approach expensive and time consuming. Numerical modelling can provide a partial solution to this problem, since it allows a fast and relatively inexpensive means of gaining insight into the parameters determining the ballistic impact response of laminated composites.

1.2 OBJECTIVE AND STRATEGY

The primary objective of the research presented in this report was to develop a numerical model to predict the interactions that occur between the helmet shell and the human head during ballistic impact. The numerical model consisted of an advanced finite element model of a ballistic helmet developed by the authors of this report as part of a previously DREV-funded project [1], and a state-of-the-art finite element head model supplied by the DGA in France.

Since the helmet and head model were developed in different finite element codes (the helmet was developed within VEC-DYNA, whereas the head model was developed within PAM-CRASH), both models were adapted to enable the simulation of ballistic impacts to the helmeted head in both codes. This way, the potential of each code to simulate ballistic impacts on helmeted heads could be evaluated and compared. Simulations were performed with the combined helmet-head model frontally impacted by

a 1.1 g FSP to predict time histories of the contact force between the head and delaminated backplane, as well as the short duration head accelerations induced by the impact.

1.3 OUTLINE

In Chapter 2, the models for the projectile, helmet, and head used in this study are presented together with the constitutive models describing the mechanical response of these structures and the corresponding material properties. Chapter 3 presents the results obtained with simulations in both PAM-CRASH and LS-DYNA. Since the constitutive model for the laminated composites was originally developed within VEC-DYNA, this material model needed to be translated to PAM-CRASH. The implementation of the composite material model in PAM-CRASH was evaluated by simulating ballistic impacts on laminated Kevlar composite panels in Section 3.2. The simulations of these panel impacts revealed that the present version of PAM-CRASH was incapable of representing the delaminations induced by the impact. Consequently, the DGA head model was translated to VEC-DYNA to simulate helmeted head impacts in Section 3.3. Conclusions and Recommendations are presented in Chapters 4 and 5, respectively. Further details concerning some aspects of the model(s) can be found in several research papers attached as an appendix to this report.

2. MODEL DESCRIPTION

2.1 MESH CHARACTERISTICS

2.1.1 PROJECTILE MESHES

Figure 1 shows the dimensions of the 1.1 g, 22 calibre chisel nose FSP (MIL-P-46593) used in this study. The FSP mesh is given in Figure 1b, which consists entirely of 8-node brick elements with single point (reduced) integration. The spin of the FSP was not modelled.

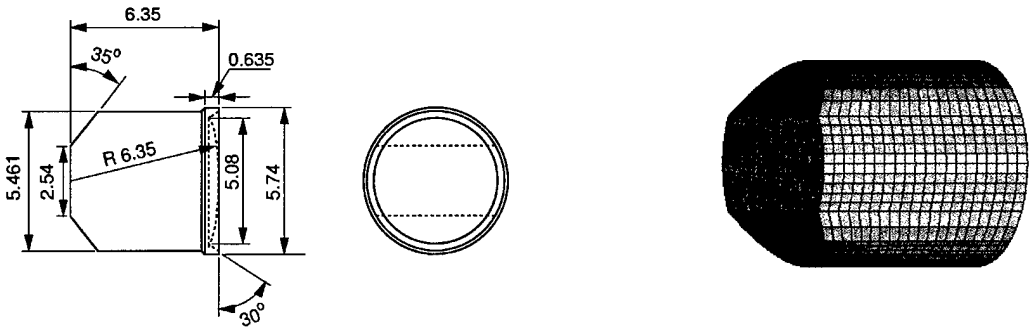

a) Dimensions b) Mesh

Figure 1: FSP dimensions and mesh.

2.1.2 HELMET MESHES

The accuracy of a finite element simulation generally improves with increased mesh density. However, a reduction in element size increases the computational costs. Since the deformation in ballistically impacted helmets was found to be localised in the impacted area [1], a gradient in mesh density was applied with sufficiently small elements in the impacted area and larger elements elsewhere. This gradient in mesh density provided sufficiently accurate results in the impacted area, without increasing the computational time too drastically. The various impact locations considered in this study required corresponding mesh gradients. The meshes developed for each impact location are presented in the following.

The geometry of the helmet was represented by measuring the position of about 16000 points on the outer surface of a PASGT helmet. The co-ordinates of these points were imported in I-DEAS Master Series 6 [2] to construct a surface representation of the helmet outer geometry. The helmet inner geometry was obtained by scaling of the outer surface such that the helmet thickness was 9.5 mm on average, which corresponded to the thickness of the actual helmet. Connecting the helmet outer and inner surfaces resulted in a 3-D representation of the helmet.

The helmet suspension system was not modelled. The effects of not modelling the suspension system were evaluated in preliminary simulations of impacts with 1.1 g FSPs.

It was found that for low mass projectiles, the effects of the impact were localised in the impacted area and that the rigid body motion of the helmet was negligible. Therefore, modeling the suspension was not deemed necessary. However, future simulations of impacts with high-mass projectiles most likely require modelling of the suspension system.

The helmet solid model was meshed in I-DEAS using brick elements. To limit the total number of elements in the helmet mesh, only part of the mesh was allowed to delaminate during the simulated impact. The size of the area for which delamination was enabled was based on previously performed impact tests on Kevlar helmets [3] and flat panels [1]. The delamination area in the helmet mesh was chosen to be larger than the delaminated area observed in these tests to avoid artificial boundary effects on the delamination growth in the simulations. The delamination area consisted of 19 layers and each layer contained 2 elements over its thickness, resulting in a total of 38 elements over the helmet thickness in the delamination area. Delamination was enabled by inserting a discrete delamination interface between adjacent layers. This delamination interface is outlined in Section 2.2.2. A custom-made piece of software was used to divide the mesh volume in the delamination areas into layers and to automatically insert delamination interfaces between adjacent layers. The mesh density was gradually decreased outside the delamination area to 20 and 10 elements over the helmet thickness. The parts with different mesh densities were connected by tied interfaces.

Frontal

Figure 2 shows the helmet mesh developed to simulate frontal impacts, together with a close-up view of the refined mesh in the impacted area.

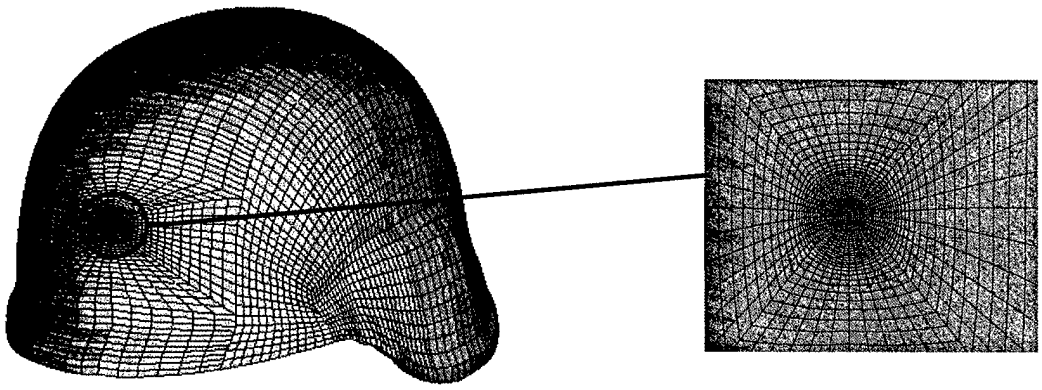

Figure 2: Helmet mesh for frontal impacts.

Rear

The helmet mesh used in simulations of rear impacts is presented in Figure 3. Similar to the mesh shown in Figure 2, this mesh is refined in the impact area and the element size increases outside this area.

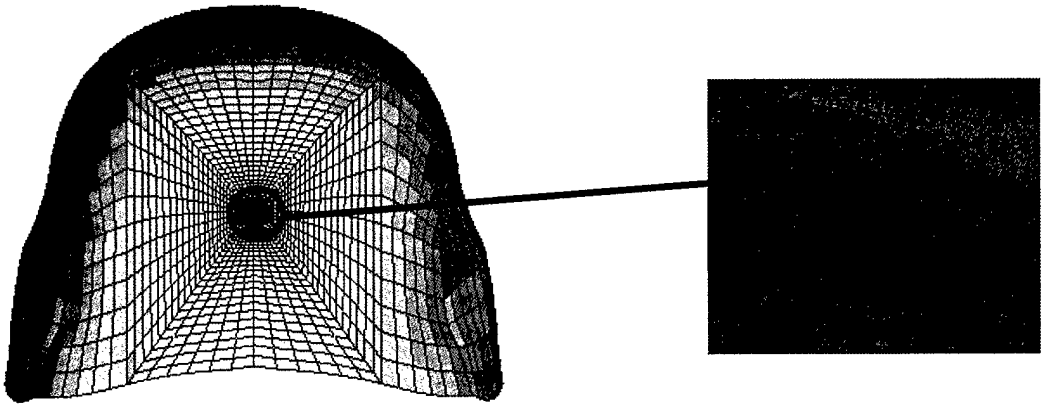

Figure 3: Helmet mesh for rear impacts.

2.1.3 DGA HEAD MODEL

Mesh

A three-dimensional finite element model of a 50th percentile human head was used for this study. The model was originally developed at Wayne State University (WSU) [4] and later modified by the ESI group and the DGA, respectively. The model contains the main anatomical components of the human head, including a three-layered skull (inner and outer table, diploe), facial bones, meninges (falx, tentorium, pia), CSF, venous sinuses, cerebrum, cerebellum, brain stem, ventricles. The final version of the head model as obtained from the DGA is presented in Figure 4.

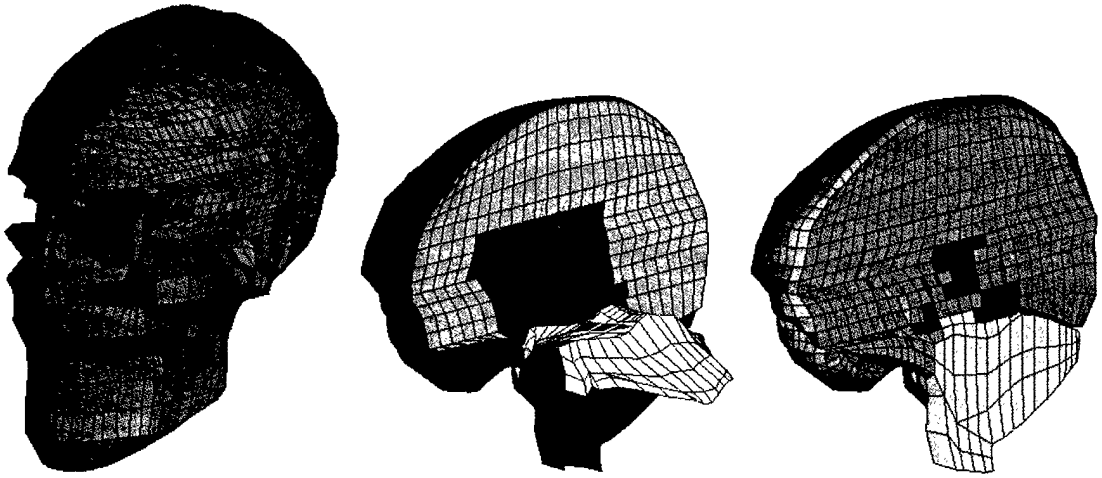

Skull Meninges Brain

Figure 4: DGA head model.

The part of the skull covering the brain (the neurocranium) is modelled as a three-layered sandwich structure with a hard outer and inner shell (outer and inner tables) covering the porous diploe. In the head model, the inner and outer table were modelled with shell elements, whereas the diploe was modelled by solid elements. The facial bones were only modelled to accurately represent the inertial properties of the human head and were represented by shell elements in the model. The CSF is a fluid layer separating the brain from the skull. The meninges (falx, tentorium, pia) are tough membranes inside the head. The pia covers the entire brain, the falx separates both brain hemispheres, and the tentorium separates the cerebrum from the cerebellum. The brain consists of the cerebrum, cerebellum, and brainstem. The ventricles are fluid-filled cavities inside the brain.

The original model developed by WSU was validated against the intracranial pressure data obtained by Nahum *et al.* [5]. However, the changes made by ESI and the DGA were not validated, although the DGA used the mesh to simulate impact tests on gel-filled human skulls.

A thorough check of the DGA head model revealed a considerable number of elements that were highly deformed in their initial state. These poorly defined elements affect the accuracy of model, especially if they are located in areas with high deformations. Most of these elements were located in the diploe and CSF part of the mesh and were 3D elements with less than 8 nodes. An example of two of these elements is given in Figure 5. These elements seemed to be major causes of numerical instabilities such as hourglassing. Therefore, these elements need to be adjusted or even removed if necessary. Modifying the head model was not part of the current project and, therefore, these adjustments were left for a future project.

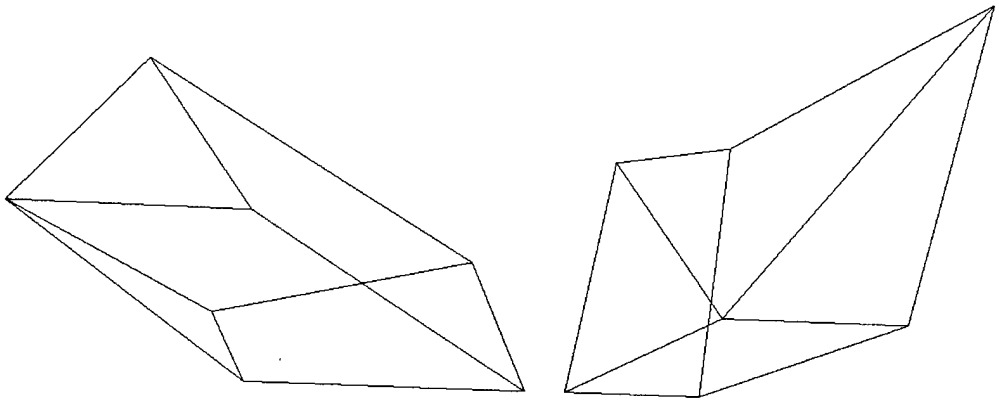

Figure 5: Example of poorly defined elements in DGA Head Model.

Skull-Brain interface

The CSF is a layer of fluid separating the brain from the skull, acting as a natural shock absorber for the brain and an interface enabling relative motion between the skull and the brain. Two different approaches are commonly used to model the skull-brain interface. One approach models the CSF as a solid with a very small shear modulus, forcing the compliant CSF layer to accommodate relative skull-brain motion [6]-[9]. The other

approach uses a contact interface to allow relative motion between the skull and the brain [10]-[17].

The DGA Head Model used the latter approach with a contact interface between the CSF layer and the inner table. The sliding interface was only capable of transmitting compressive forces between CSF and the inner table. The CSF would separate from the inner table once a tensile force existed between the two structures, resulting in a gap between the CSF and the inner table. This is a drawback of the sliding interface, since in a real human head no gap will occur between the CSF and the inner table.

Foramen Magnum

The foramen magnum is a large opening at the base of the skull that facilitates continuity between the brain and the spinal cord at the head-neck junction. The foramen magnum is thought to act as a pressure release mechanism for the brain. The foramen magnum is most commonly modelled by means of a contact interface, allowing the CSF to slide without friction along the foramen magnum [13]-[17]. This approach was also used in the DGA model.

2.2 CONSTITUTIVE MODELS

2.2.1 PROJECTILE MATERIALS

The 1.1 g FSP was modelled as an elastic-plastic material with isotropic hardening. The material parameters are given in Table 1.

Table 1: Material properties adopted for 1.1 g FSP.

E [GPa]	ν [-]	S_y [MPa]	H [MPa]
206.8	0.3	1034.2	685.0

E: Young's modulus ν: Poisson's ratio
S_y: yield strength H: hardening modulus

2.2.2 HELMET MATERIALS

Material Model

Penetration failure, fibre breakage, matrix cracking, and delamination are generally considered to be the principal damage mechanisms in ballistically impacted laminates [6]-[20]. In general, these damage modes interact and are strongly dependent on the impact conditions [21]. A post-failure damage model has been previously developed by the authors of this report to predict the response of laminated composites to ballistic impact [1]. The damage model was based on Continuum Damage Mechanics (CDM) theory [23], [24] and was implemented in the explicit, non-linear three-dimensional finite element code VEC-DYNA [25].

A distinction was made between intralaminar and interlaminar damage modes. The intralaminar damage modes (fibre breakage, matrix cracking, penetration failure) were modelled within the element constitutive routines and implemented in a user-defined material subroutine. The interlaminar failure mode included delamination and was treated using discrete interfaces inserted between layers of elements, allowing the formation of a discrete delaminated backplane during the final stages of the laminate penetration process. The following will give a concise description of the composite damage model. For a more extensive description, the reader is referred to [1].

Intralaminar Damage

The onset and growth of intralaminar damage was predicted using strain-based damage criteria, relating the relevant strain measures to corresponding critical strains:

$$f_k = \sum \left[\left(\frac{\varepsilon_{ij}}{\varepsilon_{fij}} \right)^{m_k} \right] - r_k \geq 0 : \text{damage} \tag{1}$$

where $k=1,4$ denote the damage mode, i,j the strain directions ($1,2$: in-plane; 3: transverse), ε_{ij} the strain components, ε_{fij} the corresponding failure strains, m_k the damage exponents, and r_k the damage thresholds. The damage modes, k, ranged from in-plane tensile (1,2), compressive penetration (3), and shear penetration (4). Since only woven laminated composites were considered in this study, in-plane tensile damage corresponded to fibre breakage in both weave directions. An element erosion algorithm was applied to simulate cratering of the laminate by the projectile for elements failing in either the compressive or shear penetration mode. The failure strains used in the above damage criteria were obtained from the appropriate stress-strain relations for the composite laminate through:

$$\varepsilon_{fij} = \frac{S_{ij}}{E_{ij}} \tag{2}$$

where S_{ij} represent the strength values and E_{ij} are the corresponding stiffness values (Young's or shear modulus).

Once either of the above criteria is exceeded, the onset or growth of damage is related to stiffness losses in the material by the damage variables w_{ij}:

$$\begin{aligned} E_{ij} &= (1 - w_{ij}) E_0 \\ w_{ij} &= 1 - \exp\left[\frac{-1}{m_k e} \left(\frac{\varepsilon_{ii}}{\varepsilon_{fii}} \right)^{m_k} \right] \end{aligned} \tag{3}$$

where E_0 are the undamaged stiffness parameters. A graphical representation of the effect of progressive damage on the stiffness variables and the effect of the damage exponent m are given in Figure 6.

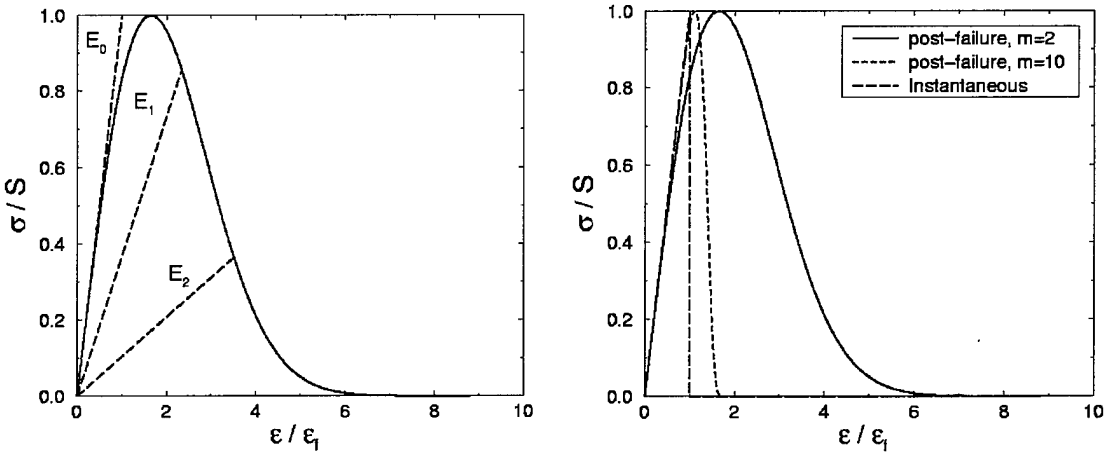

a) Effect of post-failure model on stiffness b) Effect of damage exponent *m*

Figure 6: Post-failure damage model.

The various damage modes presented in Equation 1 were coupled. The damage coupling was such that in case of tensile damage (modes 1 and 2), stiffness reduction occurred in the loading direction and in all shear directions. For the penetration damage modes (modes 3 and 4), the damage coupling was chosen such that all stiffness values were reduced as soon as damage grew in either of the two penetration modes. The stiffness matrix was updated according to changes in the damage variables w_{ij}.

Interlaminar Damage

The interlaminar failure mode included delamination and was simulated using discrete interfaces inserted between each ply of the laminate mesh. The discrete delamination interface was based on an existing contact algorithm in LS-DYNA and can be visualised by springs that resist motion between adjacent layers. The discrete delamination interface incorporates two different modes: the delamination and penetration mode.

The delamination mode is activated when tensile and/or shear forces exist in the interface. The delamination interface resists these forces until the following failure criterion is exceeded:

$$F_{delam} = \left(\frac{\sigma_n}{S_n}\right)^2 + \left(\frac{\sigma_s}{S_s}\right)^2 - 1 \geq 0 : \text{failure} \qquad (4)$$

where σ_n and σ_s are the normal and shear interface stresses, respectively, and S_n and S_s the corresponding strength values. When the delamination criterion is exceeded, the interface no longer resists separation of the connected plies, simulating inter-ply cracking. This treatment of delamination allowed the formation of a discrete delaminated backplane during the final stages of the laminate penetration process.

The penetration mode of the delamination interface is activated when the nodes in the interface penetrate the opposing elements. The interface detects this penetration and moves the penetrating nodes back out of the elements. The penetration mode of the delamination interface remains active once the interface has failed in the delamination

mode. This way, the delaminated plies are prevented from penetrating each other when the interlaminar crack closes. As was mentioned previously, elements that fail in either the compressive or shear penetration mode are deleted from the mesh to simulate the formation of a crater by the projectile. When this happens, the delamination interface is updated to remove those interface sections that are attached to the deleted elements.

Material Properties

The ballistic helmets considered in this study were fabricated from woven aramid (Kevlar-29) fabric laminae embedded in a PVB phenolic resin (MIL-C-44050, MIL-H-44099A). Material properties were obtained from data found in the literature [1], which were modified to obtain closer agreement with experimental data from ballistic impact tests on flat panels made of the same material as the helmets. The adopted values for the material properties used in the simulations of the ballistic impacts on the Kevlar helmets are summarised in Table 2 and Table 3.

Table 2: Elastic properties adopted for woven Kevlar in helmet model.

$E_{11,22}$ [GPa]	E_{33} [GPa]	ν_{21} [-]	$\nu_{31,32}$ [-]	G_{12} [GPa]	$G_{23,31}$ [GPa]	ρ [g/cm^3]
18.5	6.0	0.25	0.33	0.77	2.715	1.23

E: Young's modulus ν: Poisson's ratio
G: shear modulus ρ: density

Table 3: Strength properties adopted for woven Kevlar in helmet model.

$S_{11,22}$ [MPa]	S_{33} [MPa]	S_{12} [MPa]	$S_{23,31}$ [MPa]	S_n [MPa]	S_s [MPa]
555.0	1200.0	77.0	1086.0	34.5	9.0

2.2.3 HEAD MATERIALS

Since the head model was originally developed within PAM-CRASH, this section will focus on the PAM-CRASH material models used to represent the components comprising the head. The VEC-DYNA material models used for the translation of the head model to VEC-DYNA are presented in Section 2.3. Since the various structures comprising the head differ considerably in their mechanical response, a number of different material models were used in the DGA head model. The material properties for the various components of the head model are given in Table 4-Table 6. These material models and properties were based on data published in literature

Table 4: Components in head model with elastic plastic hydrodynamic solid properties (PAM-CRASH material model 7)

Structure	ρ [g/mm^3]	G [GPa]	S_y [GPa]	H [GPa]	T [GPa]	C1 [GPa]
CSF	1.04e-03	0.002	1.0e+04	1.0e-05	-1.0e+08	0.219

ρ: density H: hardening modulus
G: shear modulus T: tension cut-off
S_y: yield strength equation of state constant

Table 5: Components in head model with elastic plastic solid properties (PAM-CRASH material model 1)

Structure	ρ [g/mm^3]	G [GPa]	S_y [GPa]	H [GPa]	K [GPa]
Sinus Ventricles	1.04e-03	5.0e-07	10.0	1.49e-05	0.219
White matter Brainstem	1.04e-03	2.68e-04	2.0	5.0e-05	0.349
Grey matter	1.04e-03	1.68e-04	2.0	5.0e-05	0.219
Diploe	1.75e-03	1.1	1.0e+10	1.0e-07	1.598

ρ: density H: hardening modulus
G: shear modulus K: bulk modulus
S_y: yield strength

Table 6: Components in head model with elastic shell properties (PAM-CRASH material model 101)

Structure	ρ [g/mm^3]	E [GPa]	ν [-]
Tentorium Dura-sinus Falx	1.133e-03	0.0315	0.45
Pia	1.133e-03	0.0115	0.45
Inner table Outer table	3.0e-03	5.465	0.22
Face	3.0e-03	5.54	0.22

ρ: density ν: Poisson's ratio
E: Young's modulus

2.3 TRANSLATION OF HEAD MODEL TO VEC-DYNA

The head model was translated from the original PAM-CRASH format to the VEC-DYNA format so that it could be run in VEC-DYNA. This translation was performed by a custom-made piece of software. When the translated head model was run in VEC-DYNA, problems were encountered which were related to the element connectivity of a number of elements. Further examination of these elements revealed that they all were solid elements with less than 8 nodes (i.e., 5, 6, or 7 nodes). VEC-DYNA does allow 6-noded solids, but the element connectivity of these elements differs from that in PAM-CRASH. The custom-made translator was modified so that the 6-noded solids were translated to the correct element connectivity. Contrary to PAM-CRASH, VEC-DYNA does not allow 5- or 7-noded solid elements. The custom-made translator was modified so that the 5- and 7-noded solids in PAM-CRASH were translated to degenerated solid elements (8 nodes) in VEC-DYNA by defining 2 or 3 coincident nodes. Once these changes were made, the translated head model could be run in VEC-DYNA.

The numbering and input format of the material models in VEC-DYNA differ from those in PAM-CRASH. Therefore, the material models used in PAM-CRASH for the various components of the head model needed to be transferred to similar material models in VEC-DYNA. Table 7-Table 9 give the VEC-DYNA representation of the PAM-CRASH material models given in Table 4-Table 6.

Table 7: Components in head model with elastic plastic hydrodynamic solid properties (VEC-DYNA material model 10)

Structure	ρ [g/mm^3]	G [GPa]	σ_0 [GPa]	E_h [GPa]	P_c [GPa]	C1 [GPa]
CSF	1.04e-03	0.002	1.0e+04	1.0e-05	-1.0e+08	0.219

ρ: density
G: shear modulus
σ_0: yield strength
E_h: hardening modulus
P_c: pressure cut-off
C1: equation of state constant

Table 8: Components in head model with isotropic elastic plastic properties (VEC-DYNA material model 12)

Structure	ρ [g/mm^3]	G [GPa]	S_y [GPa]	E_h [GPa]	K [GPa]
Sinus Ventricles	1.04e-03	5.0e-07	10.0	1.49e-05	0.219
White matter Brainstem	1.04e-03	2.68e-04	2.0	5.0e-05	0.349
Grey matter	1.04e-03	1.68e-04	2.0	5.0e-05	0.219
Diploe	1.75e-03	1.1	1.0e+10	1.0e-07	1.598

ρ: density
G: shear modulus
S_y: yield strength
E_h: hardening modulus
K: bulk modulus

Table 9: Components in head model with elastic properties (VEC-DYNA material model 1)

Structure	ρ [g/mm^3]	E [GPa]	ν [-]
Tentorium Dura-sinus Falx	1.133e-03	0.0315	0.45
Pia	1.133e-03	0.0115	0.45
Inner table Outer table	3.0e-03	5.465	0.22
Face	3.0e-03	5.54	0.22

ρ: density
E: Young's modulus
ν: Poisson's ratio

3. SIMULATIONS

3.1 IMPLEMENTATION OF COMPOSITE DAMAGE MODEL IN PAM-CRASH

The composite damage model described in Section 2.2.2 was originally implemented in VEC-DYNA [1]. Since the DGA Head Model was developed within the PAM-CRASH finite element code, the damage model was implemented in PAM-CRASH to enable the simulation of ballistic impacts to helmeted heads in PAM-CRASH. The existing composite damage model in PAM-CRASH was modified to represent the damage model described in Section 2.2.2. The required material properties, as given in Table 2 and Table 3, are entered in PAM-CRASH as PLY-data according to the definitions presented in Table 10.

Table 10: Definition of material properties for composite damage model implementation in PAM-CRASH.

columns	CARD 3	CARD 4	CARD 5	CARD 6	CARD 7
1-10	E_{11}	G_{12}	ε_{f11}	ε_{f22}	ε_{f33}
11-20	E_{22}	G_{23}	m_1	m_2	m_3
21-30	E_{33}	G_{13}	t_1	t_2	t_3
31-40		ν_{12}	n_1	n_2	n_3
41-50		ν_{23}			
51-60		ν_{13}			

3.2 SIMULATION OF PANEL IMPACTS IN PAM-CRASH

A large number of ballistic impact tests on flat Kevlar panels with a range of projectiles and impact velocities were simulated in VEC-DYNA to evaluate the accuracy of the composite damage model [1]. These simulations showed that the model was capable of accurately predicting the experimental data. The simulations were repeated with the implementation of the composite damage model in PAM-CRASH to analyse the potential of PAM-CRASH to simulate ballistic impacts.

Figure 7 presents the result of a PAM-CRASH simulation of a 1.1 g FSP impacting a flat Kevlar panel at 586 m/s. The figure shows that the erosion algorithm in PAM-CRASH works properly, resulting in the FSP creating a crater in the panel mesh. However, Figure 7 shows that adjacent layers penetrated each other, indicating the delamination interface was not working properly. The delamination interface was based on slideline type 32 in PAM-CRASH, which is similar to the tied interface in VEC-DYNA upon which the original delamination interface was based.

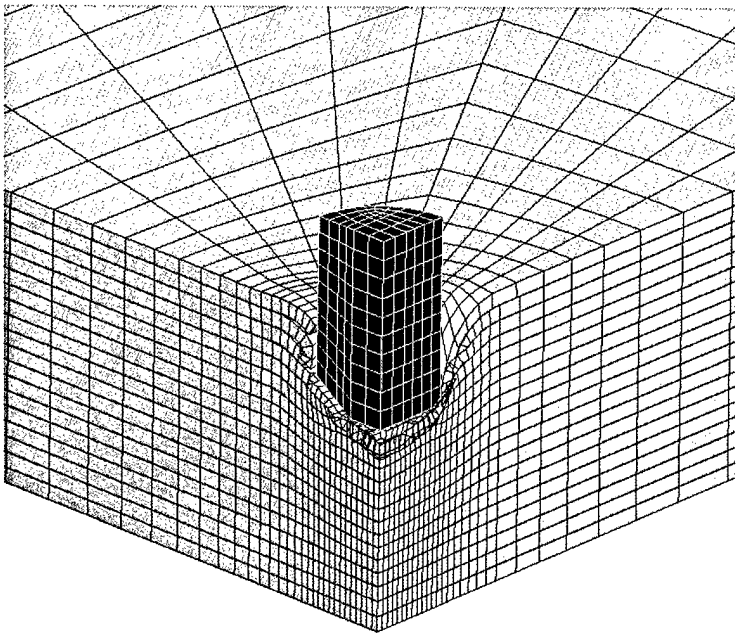

Figure 7: PAM-CRASH simulation of 1.1 g FSP impacting a Kevlar flat panel at 586 m/s.

However, an important difference between the PAM-CRASH slideline 32 and the VEC-DYNA tied interface is that slideline 32 requires the definition of a contact thickness. The effects of this contact thickness are shown in Figure 8. The contact thickness represents the distance ahead of the contacting surface at which contact is detected. Detecting contact ahead of the contacting surfaces reduces the contact forces necessary to remove penetrations when the contacting surfaces approach each other at high velocities. However, the use of a contact thickness for the delamination interface requires that the adjacent layers are separated by a distance larger than the contact thickness to avoid initial penetrations.

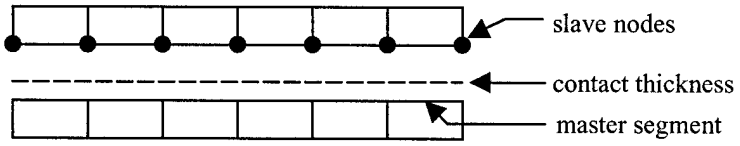

Figure 8: Contact thickness in PAM-CRASH slideline 32.

To accurately represent the bending behaviour of the laminate, the adjacent layers should be separated as little as possible. However, this small separation results in a very small contact thickness in the delamination interface. The contact thickness in front of the contacting surface is accompanied by a shadow distance behind the contacting surface, which is by default 3 times as large as the contact thickness. The contact algorithm is only active when a node is positioned between the contact thickness and the shadow distance. A small contact thickness can result in a node moving from a position in front of the contact thickness to a position behind the shadow distance within one time step. As a result, the contact is not detected and the penetration of the node is not removed.

This is the reason for the layers penetrating each other in Figure 7. As a result, PAM-CRASH was found not capable of accurately simulating ballistic impacts on laminated composites using the present Waterloo delamination interface treatment. This problem has been communicated to ESI and DGA for future action.

3.3 Simulation of Helmeted Head Impacts in VEC-DYNA

Since simulations with the composite damage model in VEC-DYNA were found to be capable of accurately predicting the ballistic impact response of flat Kevlar panels in [6], the model was applied to simulate ballistic impacts to a helmeted head. This section focuses on frontal impacts to the helmet by a 1.1 g FSP at 586 m/s. The resulting model is shown in Figure 9. As described in Section 2.1.2, the helmet suspension system was not modelled. Consequently, the helmet model was floating freely above the head.

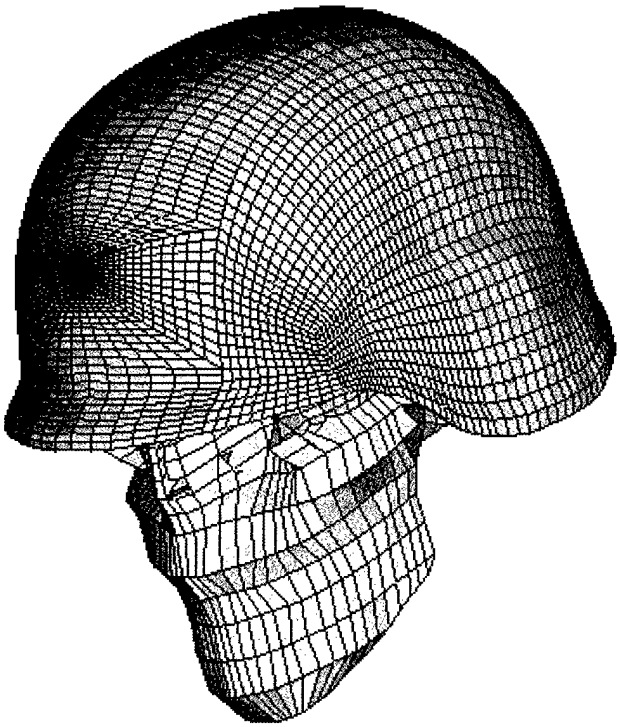

Figure 9: VEC-DYNA model of the helmeted head subjected to frontal impact.

Simulations with the model shown in Figure 9 were not successful because the number of elements and nodes exceeded VEC-DYNA's capacity. To solve this problem, the delaminating area was isolated from the helmet model and the skull was isolated from the head model. The resulting model containing the FSP, delaminating area, and skull is presented in Figure 10. We will refer to this model as the simplified helmet-head model from now on. The average stand-off between the actual helmet and the head is about 12-15 mm. However, due to the curved shape of the helmet, the stand-off is larger at the front. For the simplified helmet-head model, the stand-off between the delaminating area and the skull was about 20 mm to accommodate this larger stand-off at the front.

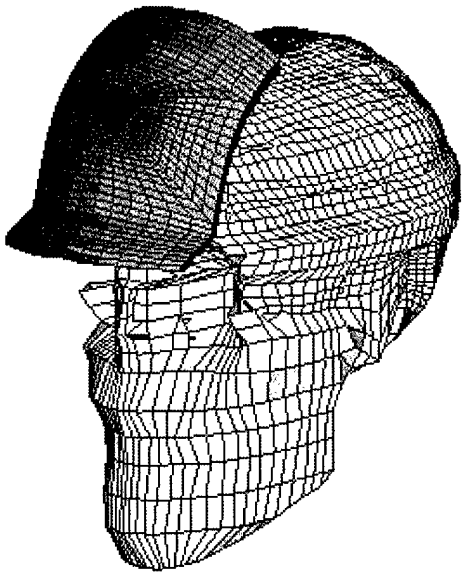

Figure 10: VEC-DYNA model of FSP, delaminating area, and skull.

Figure 11 contains a series of deformed mesh plots obtained from the simulation of a 1.1 g FSP frontally impacting the simplified helmet-head model at 586 m/s. Figure 11a shows the initial stage of the penetration process, where the projectile forms a crater in the helmet mesh by deletion of elements that failed in either of the two penetration damage modes. The Figure also shows the initiation of the backplane. Figure 11b shows the impact of the delaminated backplane with the skull, indicated by the maximum principal stresses in the skull.

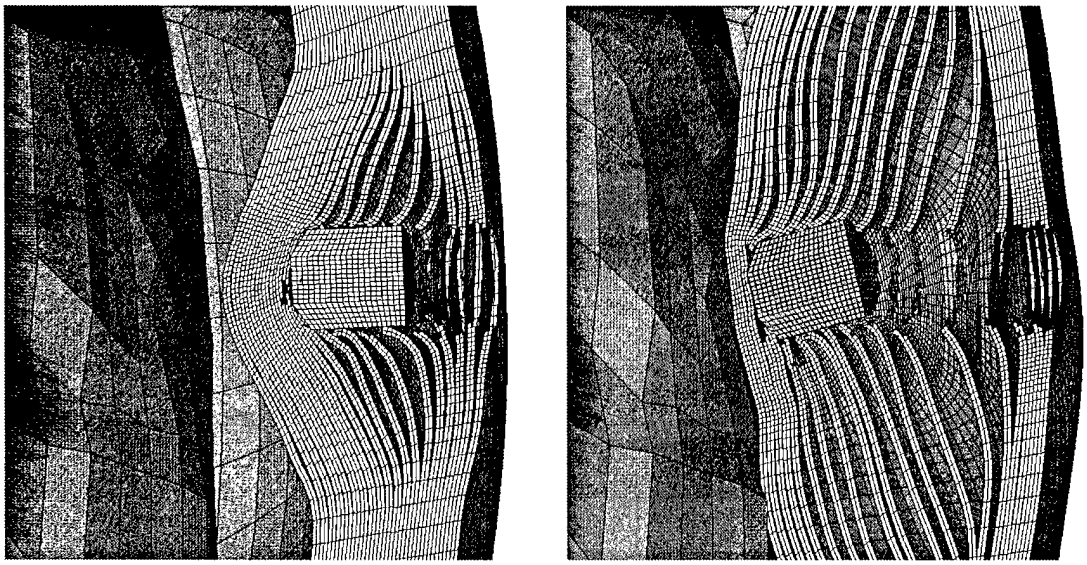

Figure 11: Deformed mesh plots obtained from simulation of a 1.1 g FSP frontally impacting a helmeted head.

Figure 12 presents the inside of the skull underneath the impacted area, indicating that the backplane penetrated the skull. This penetration error was caused by the large difference in element size between the backplane and the skull. Generally, the difference in mesh

density between contacting surfaces should not be more than a factor 2-3, which is largely exceeded by the mesh shown in Figure 12. As a result of the large difference in mesh density, the contact algorithm in VEC-DYNA was not capable of preventing the backplane from penetrating the skull. Therefore, there clearly is a need to refine the skull mesh.

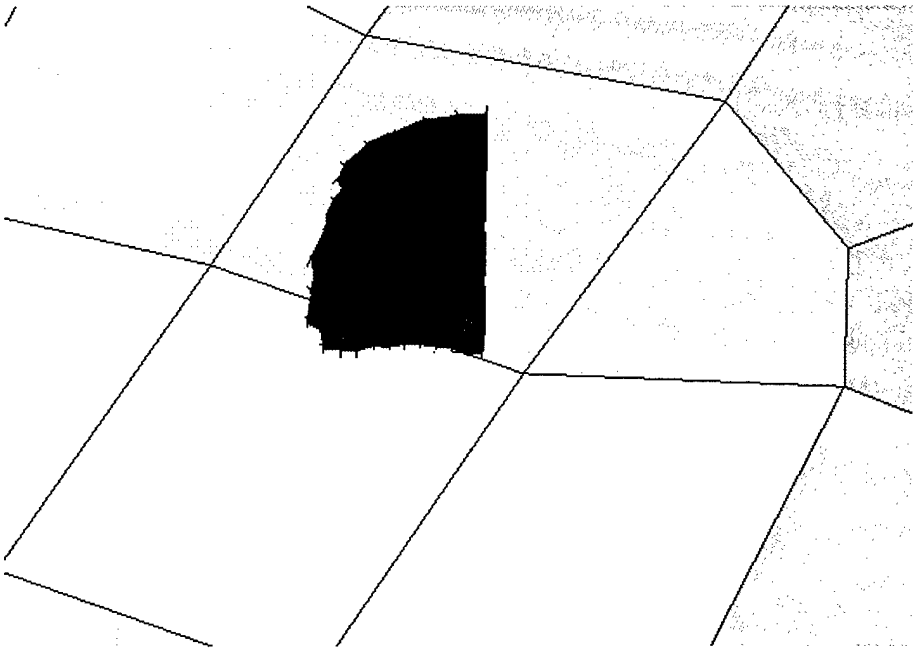

Figure 12: Backplane penetrating skull.

Other problems with the contact algorithm were found related to the VEC-DYNA contact search algorithm, which only allows a maximum of 1000 nodes in each contact interface (so-called contact search bucket). The contact search bucket includes all nodes within the volume defined by the nodes in the contact interface. In the helmet simulation, elements broke loose and moved away from the crater area. Consequently, the volume defined by the nodes in the contact interface increased as nodes moved further outwards. This can lead to more than the maximum allowable number of nodes in the search bucket of 1000, which automatically results in termination of the simulation. This problem has been solved in the currently available proprietary version of LS-DYNA. Therefore, the University of Waterloo Composite Damage Model should be implemented in LS-DYNA to enable the foregoing helmeted head simulations in LS-DYNA.

Figure 13 presents the pressure distribution in the skull resulting from the impact with the backplane. The contour plot indicates a maximum contact pressure of about 2.7 MPa in the skull.

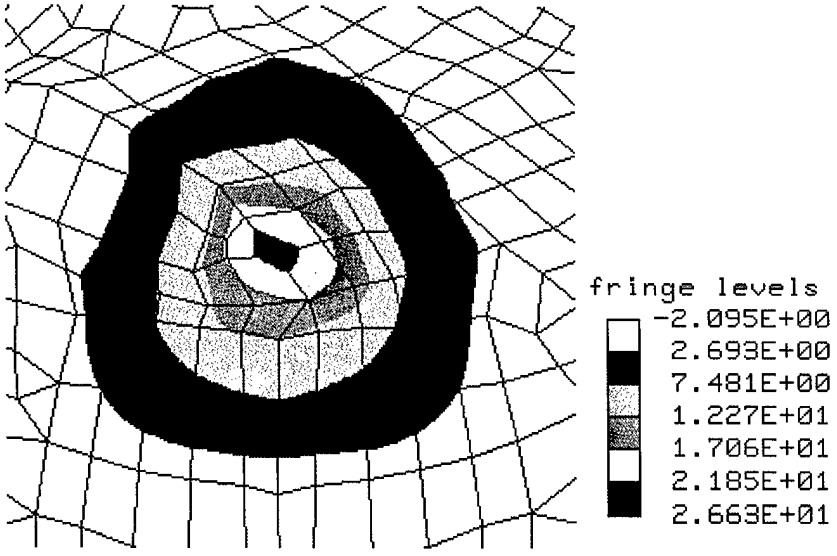

Figure 13: Contour plot of pressure distribution in the skull [MPa].

The rigid body acceleration of the skull mesh is presented in Figure 14. The figure shows that the skull acceleration is zero until the backplane impacts the skull, after which it undergoes substantial acceleration. However, it should be noted that the intracranial components were removed from the head model to speed up the simulation. When the intracranial components are included, the head will be substantially heavier, which reduces the rigid body acceleration. On the other hand, Figure 12 showed that the contact interface between the helmet interior and the skull was not working properly as a result of large differences in element sizes. Once this problem is solved, a larger portion of the backplane kinetic energy will be transferred to the skull, resulting in larger skull accelerations. The effects of including the intracranial contents and the improved helmet-skull contact definition need to be investigated in the future.

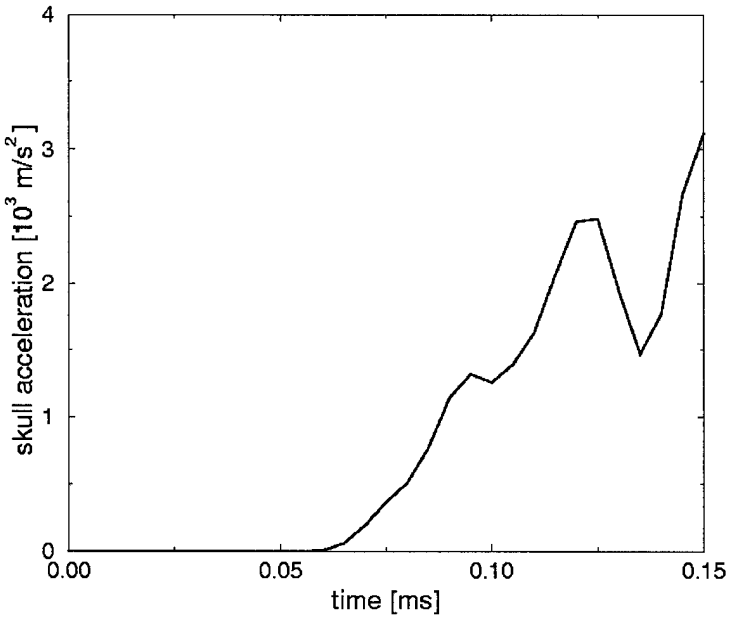

Figure 14: Head rigid body acceleration.

3.4 COMPARISON BETWEEN HELMET AND PANEL SIMULATIONS

The simulations with the helmet model were compared with previously performed simulations with flat panels [1] to check the effects of the helmet curvature on the backplane deformation. The results for impacts with a 1.1 g FSP at 586 m/s are presented in Figure 15. The figure shows that the projectile velocity and backplane displacement for the helmet and flat panel simulations are initially similar. However, the response of the helmet and panel models deviate around the point of maximum backplane displacement. At this point, the projectile is pushed back upwards by the panel backplane, whereas in case of the helmet the projectile does not move and the backplane continues to deform. Figure 15 also contains data from IMAX and VISAR measurements obtained during an impact of a 1.1 g FSP on a Kevlar panel at 586 m/s. These measurements provide an indication of the accuracy of the simulations. A more thorough evaluation of the accuracy of the panel simulations is presented in [1]. Unfortunately, similar measurements on helmets are not available.

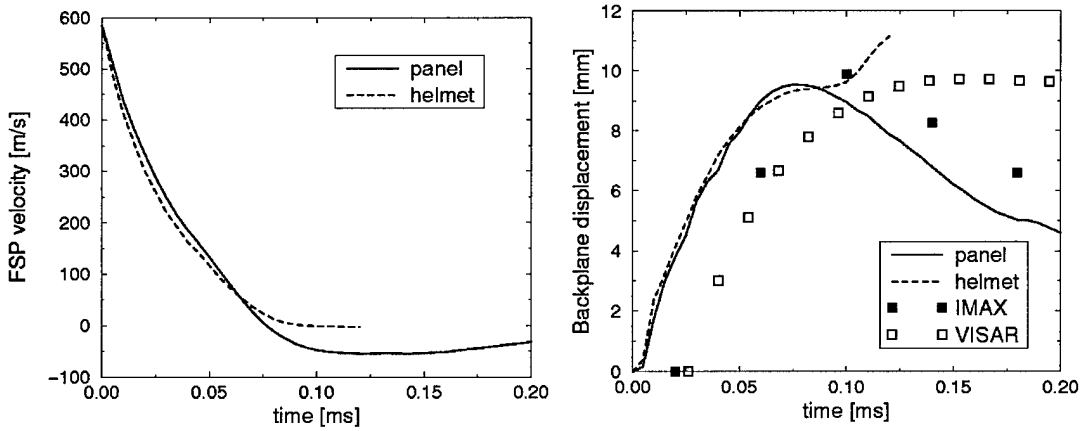

Figure 15: Comparison between simulations with flat panel and helmet impacted by 1.1 g FSP at 586 m/s.

Figure 16 presents deformed mesh plots obtained from the helmet and panel simulations. The deformed meshes were obtained at the time of maximum backplane deformation in the helmet simulation. The figure shows that for the panel simulation, the projectile does not yaw. However, in case of the helmet simulation, the projectile gets wedged inside the helmet. This explains why the projectile gets pushed upwards by the rebounding panel backplane, whereas the projectile becomes immobile in the helmet simulation.

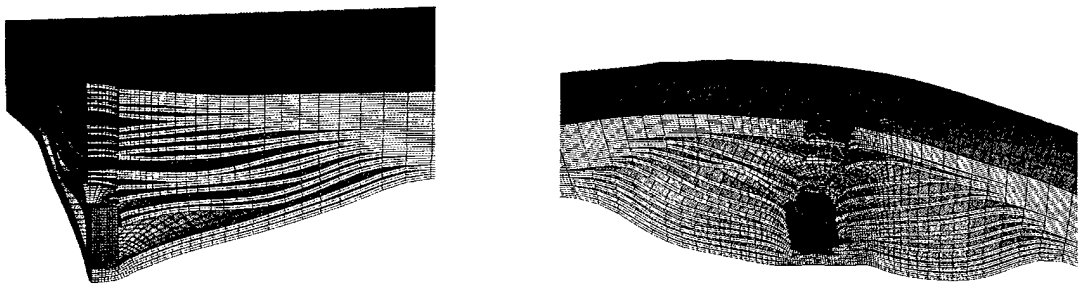

Figure 16: Deformed mesh plots of panel and helmet at time of maximum backplane deformation for helmet model.

4. CONCLUSIONS

The composite damage model was successfully implemented in PAM-CRASH. However, simulations showed that the required use of a contact thickness in the slideline algorithm made PAM-CRASH incapable of accurately predicting the ballistic impact response of laminated composites.

The DGA Head Model was translated to the VEC-DYNA format and successfully used in simulations of ballistics impacts to the helmeted head. Limitations exist in the contact treatment available in VEC-DYNA and it is desirable to perform the calculations in LS-DYNA. Discussions to implement the Waterloo delamination interface within LS-DYNA are underway with LSTC.

At present the skull model available for this work is too coarse; that is, the element size is too large to accurately capture the local gradients associated with contact with the finely meshed helmet.

5. *RECOMMENDATIONS*

1. In order to pursue simulation of impacts on helmeted heads within PAMCRASH, further effort is required to modify the delamination interface within the present PAMCRASH version to overcome the problems outlined in this report.
2. The model has successfully modelled impact of the helmet on the skull using the DGA head model VEC-DYNA. This model is based upon automotive crash requirements and is not sufficiently refined near the impact site to accurately capture local contact conditions. Techniques to automatically refine the skull mesh at any impact site of interest are required.
3. The delamination interface needs to be implemented within LS-DYNA since the current VEC-DYNA code used in this research suffers from contact limitations associated with the maximum bucket size in the contact sorting algorithm.

6. REFERENCES

[1] van Hoof J, *Modelling of impact induced delamination in composite materials,* PhD Thesis, Department of Mechanical and Aerospace Engineering, Carleton University, Ottawa, Canada, 1999.

[2] I-DEAS Master Series 6, Structural Dynamics Research Corporation, 1998.

[3] Van der Heiden N., van Bree J., *Evaluation of the behaviour of a copper liner for indentation response analyses in composite helmets under FSP impacts*, TNO Report PML 1994-A86, TNO Prins Maurits Laboratory, Rijswijk, The Netherlands.

[4] Zhou C, Khalil T, King AI, *A New Model Comparing Impact Responses of the Homogeneous and Inhomogeneous Human Brain*, Proceedings of 39th Stapp Car Crash Conference, 1995, pp. 121-137.

[5] Nahum AM, Smith RW, Ward CC, *Intracranial Pressure Dynamics During Head Impact*, Proceedings of 21st Stapp Car Crash Conference, 1977, pp. 337-365.

[6] Ruan, J.S., Khalil, T. and King, A.I., *Intracranial Response of a Three-Dimensional Human Head Finite Element Model*, Proceedings of Injury Prevention Through Biomechanics Symposium, Wayne State University, 1991, pp. 97-103.

[7] Zhou, C., Khalil, T. and King, A.I., *A New Model Comparing Impact Responses of the Homogeneous and Inhomogeneous Human Brain*, Proceedings of 39th Stapp Car Crash Conference, 1995, pp. 121-137.

[8] Zhou, C., Khalil, T. and King, A.I., *Viscoelastic Response of the Human Brain to Sagittal and Lateral Rotational Acceleration by Finite Element Analysis*, Proceedings of International Conference on the Biomechanics of Impacts, 1996, pp. 35-48.

[9] Zhou, C., Khalil, T. and King, A.I., *Head Injury Assessment of a Real World Crash by Finite Modeling*, AGRAD Conference Proceedings 597, Impact Head Injury: Responses, Mechanisms, Tolerance, Treatment and Countermeasures, 1996, pp. 8.1-8.8.

[10] Dimasi, F., Marcus, J. and Eppinger, R., *3-D Anatomic Brain Model for Relating Cortical Strains to Automobile Crash Loading*, Proceedings of 13th International Conference on Experimental Safety Vehicles, 1991, pp. 916-924.

[11] Bandak, F.A. and Eppinger, R.H., *A Three-Dimensional Finite Element Analysis of the Human Brain Under Combined Rotational and Translational Accelerations*, Proceedings of 38th Stapp Car Crash Conference, 1994, pp. 145-163.

[12] Dimasi, F., Eppinger, R.H. and Bandak, F.A., *Computational Analysis of Head Impact Response Under Car Crash Loadings*, Proceedings of 39th Stapp Car Crash Conference, 1995, pp. 425-438.

[13] Lighthall, J.W., Melvin, J.W. and Ueno, K., *Toward a Biomechanical Criterion for Functional Brain Injury*, in Proceedings of the 12th International Conference on Experimental Safety Vehicles, 1989, pp. 627-633.

[14] Ueno, K., Melvin, E., Lundquist, E. and Lee, M.C., *Two-Dimensional Finite Element Analysis of Human Brain Impact Responses: Application of a Scaling Law*, Crashworthiness and Occupant Protection in Transportation Systems, AMD-Vol. 106/BED-Vol. 13, Ed. T.B. Khalil, ASME, 1989, pp. 123-124.

[15] Trosseille, X., Tarriere, C., Lavaste, F., Guillon, F. and Domont, A., *Development of a F.E.M. of the Human Head According to a Specific Test Protocol*, in Proceedings of the 36th Stapp Car Crash Conference, 1992, pp. 235-253.

[16] Chu, C.-S., Lin, M.-S., Huang, H.-M. and Lee, M.-C., *Finite Element Analysis of Cerebral Contusion*, Journal of Biomechanics, Vol. 27(2), 1994, pp. 187-194.

[17] Kuijpers, A., Claessens, M. and Sauren, A., *The Influence of Different Boundary Conditions on the Response of the Head to Impact: A Two-Dimensional Finite Element Study*, Journal of Neurotrauma, Vol. 12, No. 4, 1995, pp. 715-724.

[18] Langlie S, Cheng, W., *A high velocity impact penetration model for thick fiber-reinforced composites*, Proceedings of the ASME Pressure Vessels and Piping Conference, Honolulu, HI, USA, July 23-27, 1989 pp. 151-158.

[19] Zhu G, Goldsmith W, Dharan C., *Penetration of laminated Kevlar by projectiles – I. Experimental investigation*, International Journal of Solids and Structures 29(4), 1992, pp. 399-420.

[20] Zhu G, Goldsmith W, Dharan C., *Penetration of laminated Kevlar by projectiles – II. Analytical model*, International Journal of Solids and Structures 29(4), 1992, pp. 421-436.

[21] Peijs T, Smetts E, Govaert L, *Strain rate and temperature effects on energy absorption of polyethylene and carbon fibres*, Advanced Composite Materials 1(1), 1994, pp. 35-54.

[22] van Hoof J, Worswick MJ, Straznicky PV, *Simulation of the backplane response of composite helmet materials under ballistic impact*, Final report for DREV contract W7701-5-1203/01-XSK, October 1999.

[23] Kachanov L, *Introduction to Continuum Damage Mechanics*, Martinus Nijhoff Publishers, Dordrecht, The Netherlands, 1986.

[24] Matzenmiller A, Lubliner J, Taylor R, *A constitutive model for anisotropic damage in fiber-composites*, Mechanics of Materials 20,1995, pp. 125-152.

[25] Livermore Software Technology Corporation, *LS-DYNA Users's Manual - Nonlinear Dynamic Analysis of Structures*, Version 950, 1999.

[26] PAM SYSTEM INTERNATIONAL SA, *PAM-CRASH Solver Reference Manual*, Version 1998.

INTERNAL DISTRIBUTION

1 – Director General

1 – Deputy Director General

1 – Head, Weapon Effects Section

6 – Document Library

1 – Dr. K. Williams

1 – Dr. D. Nandlall

1 – M. Szymczak

1 – G. Pageau

1 – D. Bourget

1 – M. Bolduc

EXTERNAL DISTRIBUTION

1 – DRDKIM
1 – DRDKIM (unbound copy)

1 – DRDC

1 – DSTL
1 – DSTL 2

1 – DCIEM
Attn: Dr. Frim

1 – DLR 5

1 – DSSPM 8

1 – National Library of Canada

1 – CISTI

1 – DTIC

1 – DSP/STTC
4, rue de la Porte D'Issy
75015 Paris
France
Attn: Mr. Jean-Claude Sarron

1 – TNO Prins Maurits Laboratiry
Lange Kleiweg 137
P.O. Box 45
2280 AA Rijswijk
The Netherlands
Attn: Dr. I.J. van Bree

1 – Livermore Software Technology Corporation
7374 Las Positas Road
Livermore, California
USA 94550
Attn: Dr. J.O. Halquist

DOCUMENT CONTROL DATA

1. ORIGINATOR (name and address)	2. SECURITY CLASSIFICATION (Including special warning terms if applicable)
J. van Hoof and M.J. Worswick Department of Mechanical Engineering University of Waterloo Waterloo, Ontario	UNCLASSIFIED

3. TITLE (Its classification should be indicated by the appropriate abbreviation (S, C, R or U)

Combining Head Models with Composite Helmet Models to Simulate Ballistic Impacts

4. AUTHORS (Last name, first name, middle initial. If military, show rank, e.g. Doe, Maj. John E.)

van Hoof, J. and Worswick, M.J.

5. DATE OF PUBLICATION (month and year)	6a. NO. OF PAGES	6b. NO. OF REFERENCES
November 2000	30	26

7. DESCRIPTIVE NOTES (the category of the document, e.g. technical report, technical note or memorandum. Give the inclusive dates when a specific reporting period is covered.)

Contract Final Report

8. SPONSORING ACTIVITY (name and address)

DRDB

9a. PROJECT OR GRANT NO. (Please specify whether project or grant)	9b. CONTRACT NO.
Work Unit 2cb15	W7701-8-1713

10a. ORIGINATOR'S DOCUMENT NUMBER	10b. OTHER DOCUMENT NOS
DREV CR 2000-160	N/A

11. DOCUMENT AVAILABILITY (any limitations on further dissemination of the document, other than those imposed by security classification)

- ☒ Unlimited distribution
- ☐ Contractors in approved countries (specify)
- ☐ Canadian contractors (with need-to-know)
- ☐ Government (with need-to-know)
- ☐ Defense departments
- ☐ Other (please specify)

12. DOCUMENT ANNOUNCEMENT (any limitation to the bibliographic announcement of this document. This will normally correspond to the Document Availability (11). However, where further distribution (beyond the audience specified in 11) is possible, a wider announcement audience may be selected.)

Same as 11

13. ABSTRACT (a brief and factual summary of the document. It may also appear elsewhere in the body of the document itself. It is highly desirable that the abstract of classified documents be unclassified. Each paragraph of the abstract shall begin with an indication of the security classification of the information in the paragraph (unless the document itself is unclassified) represented as (S), (C), (R), or (U). It is not necessary to include here abstracts in both official languages unless the text is bilingual).

Numerical modelling of a helmeted head undergoing ballistic impact has been undertaken using a number of finite element codes and models. The University of Waterloo composite helmet model has been combined with a model of the human head, originally developed for automotive crash studies and extended to consider trauma due to ballistic impact. Two head models were considered. Initially, the Délégation Générale pour l'Armement (DGA) head model was run within the PAMCRASH finite element code. This choice of code and head model was adopted to enable collaborative exchange with the French DGA and required implementation of the Waterloo composite model within PAMCRASH. Incompatibilities were identified mid-way through the implementation process; however, modifications to PAMCRASH to allow proper treatment of the delamination algorithm have not been made available by ESI to date.

As a work-around to the problems encountered in PAMCRASH, it was decided to run the simulations within VEC-DYNA. To facilitate this work, DGA has allowed the university to convert their head model to VEC-DYNA format. Once the conversion was completed, it has been possible to perform the required simulations and preliminary predictions of the contact forces resulting from the impact of the backplane with the skull have been obtained.

At present, the existing head model requires further mesh refinement in the vicinity of the impact sites to accurately capture local contact conditions. There is also a need to migrate the delamination interface from VEC-DYNA to the proprietary version of LS-DYNA. The skull re-meshing task is underway in follow-on work in an internally funded project at Waterloo while a joint project with UBC under DREV funding will address the delamination interface implementation.

14. KEYWORDS, DESCRIPTORS or IDENTIFIERS (technically meaningful terms or short phrases that characterize a document and could be helpful in cataloguing the document. They should be selected so that no security classification is required. Identifiers, such as equipment model designation, trade name, military project code name, geographic location may also be included. If possible keywords should be selected from a published thesaurus, e.g. Thesaurus of Engineering and Scientific Terms (TEST) and that thesaurus-identified. If it is not possible to select indexing terms which are Unclassified, the classification of each should be indicated as with the title.)

Numerical Simulation
Finite Element
Hydrocode Simulation
LS-DYNA3D
Helmet
Kevlar
Backplane Deformation
Ballistic Response
Biomechanical Modeling
Head Trauma